

## End of aging as a probe of finite-size effects near the spin-glass transition temperature


Gregory G. Kenning,<sup>1</sup> Daniel M. Tennant,<sup>1,2,3</sup> Christina M. Rost,<sup>1</sup> Fagner Garrote da Silva,<sup>1</sup> Brian J. Walters,<sup>1</sup> Qiang Zhai,<sup>2</sup> David C. Harrison,<sup>4</sup> E. Dan Dahlberg,<sup>4</sup> and Raymond L. Orbach<sup>2</sup>

<sup>1</sup>*Department of Physics, Indiana University of Pennsylvania, Indiana, Pennsylvania, 15705, USA*

<sup>2</sup>*Texas Materials Institute, The University of Texas at Austin, Austin, Texas 78712, USA*

<sup>3</sup>*Institute of Quantum Computing, The University of Waterloo, Waterloo, Ontario, Canada, N2L 3G1*

<sup>4</sup>*School of Physics and Astronomy, The University of Minnesota, Minneapolis, Minnesota, 55455, USA*

 (Received 22 February 2018; revised manuscript received 12 August 2018; published 28 September 2018; corrected 8 April 2019)

We have measured the growth of the spin glass correlation length through the aging effect. Measurements were made on bulk  $\text{Cu}_{0.95}\text{Mn}_{0.05}$  and a  $\text{Cu}_{0.88}\text{Mn}_{0.12}$  thin film multilayer with CuMn layer thicknesses of 4.5 nm separated by 60-nm Cu layers. As the glass temperature  $T_g$  is approached ( $0.9T_g < T < 0.96T_g$ ) in the bulk sample, we find that the waiting time effect (as measured by the time associated with the inflection point of the decay) as a function of increasing temperature, shifts to shorter timescales. For  $T > 0.96T_g$ , there is no waiting time effect on the magnetization decay. In the temperature region  $0.96T_g - 1.00T_g$ , all decays collapse onto a single decay curve indicating an end of aging even for long waiting times ( $t_w = 10\,000\text{s}$ ). For the thin film, all effects due to the waiting time disappear at around  $0.89T_f$ , where  $T_f$  is the freezing temperature marking the onset of irreversibility. These results are interpreted in terms of the spin glass correlation length saturating at a constant value after reaching a characteristic length scale, either the size of the crystallites in the bulk, or the thickness of the 4.5-nm film.

DOI: [10.1103/PhysRevB.98.104436](https://doi.org/10.1103/PhysRevB.98.104436)

### I. INTRODUCTION

Despite more than 40 years [1,2] of theoretical and experimental effort, a complete understanding of the 3D spin glass state has remained elusive. Spin glasses have an interesting phase transition evidenced by strong time dependencies in the magnetic properties at and below the transition temperature. In this sense, many spin glass properties appear glassy in nature. To date, direct measurements of a correlation length  $\xi(t, T)$  have been absent. For example, neutron scattering experiments reveal the order parameters for ferro- and anti-ferromagnets, but not for the spin glass state [3].

There is, however, another avenue for studying spatial correlations in spin glasses. The spin glass state exhibits very large finite size effects [4]. Systematic studies of CuMn multilayer films of decreasing spin glass thickness have shown the apparent freezing temperature,  $T_f$ , to decrease as the logarithm of the film thickness,  $T_f \sim \ln(\mathcal{L})$ , for conventional measurement timescales. It was shown that  $T_f \sim \ln(\mathcal{L})$  for different concentrations and different length scales could be collapsed onto a single curve if scaled with the parameter  $\mathcal{L}/a_0$  where  $a_0$  is the average Mn-Mn separation [5]. The length dependence of  $T_f(\mathcal{L}/a_0)$  is apparently universal, depending only on film thickness and the bulk transition temperature  $T_g$ , and independent of Mn concentration [4], constituents [6], and whether the layered spin glass is metallic or semiconductor [7].

Our work demonstrates the relationship between aging and the correlation length experimentally, without resorting to a theoretical model. We have been able to quantitatively assign the end of aging to the establishment of a quasiequilibrium spin glass state when the correlation length has reached  $\mathcal{L}$ , the

thickness of CuMn thin films. We believe that the apparent universality of the finite size effects justifies our comparison of bulk dynamics with thin film dynamics with different concentrations. The comparison between bulk and thin film samples forms the basis of our conclusions.

The spin glass state exhibits very large finite size effects, resulting from a lower critical dimension,  $d_\ell$ , of the spin glass state lying between two and three dimensions [8–10]. This means that, for a thin film, the growth of the correlation length perpendicular to the film,  $\xi_\perp(t, T)$ , stops at the thickness of the film,  $\mathcal{L}$ , at a time we shall designate as the crossover time,  $t_{co}$ . Because  $\xi_\perp(t, T)$  is now fixed, the correlation length parallel to the film is associated with a reduction in dimensionality to  $\mathcal{D} = 2$ . The parallel correlation length,  $\xi_\parallel(t, T)$ , is driven by a  $T = 0\text{K}$  transition temperature [11], but renormalized by the correlations contained within the  $\xi_\perp(t, T) = \mathcal{L}$  length scale [12]. The correlated volume is then “pancake-like” with thickness  $\mathcal{L}$  and width  $\xi_\parallel(T)$ , as confirmed by recent experiments [13]. Because the correlated volume is limited by these two length scales, there is no further growth of  $\xi$  in time for  $t > t_{co}$ . Therefore any dynamics that depend on aging would cease as long as the external conditions (e.g., magnetic field, temperature) are unchanged. The end of aging can then be used as a direct measure of the growth of  $\xi(t, T)$  without the use of a model, as noted above. In experimental terms, dynamics that depend upon aging would cease to change for times  $t > t_{co}$ .

The conventional method of determining the spin glass transition temperature is the demarcation of the field-cooled (FC) and zero-field-cooled (ZFC) magnetizations. This signals the onset of irreversibility, and entry into the spin glass phase. We refer to this temperature in this manuscript as  $T_g$

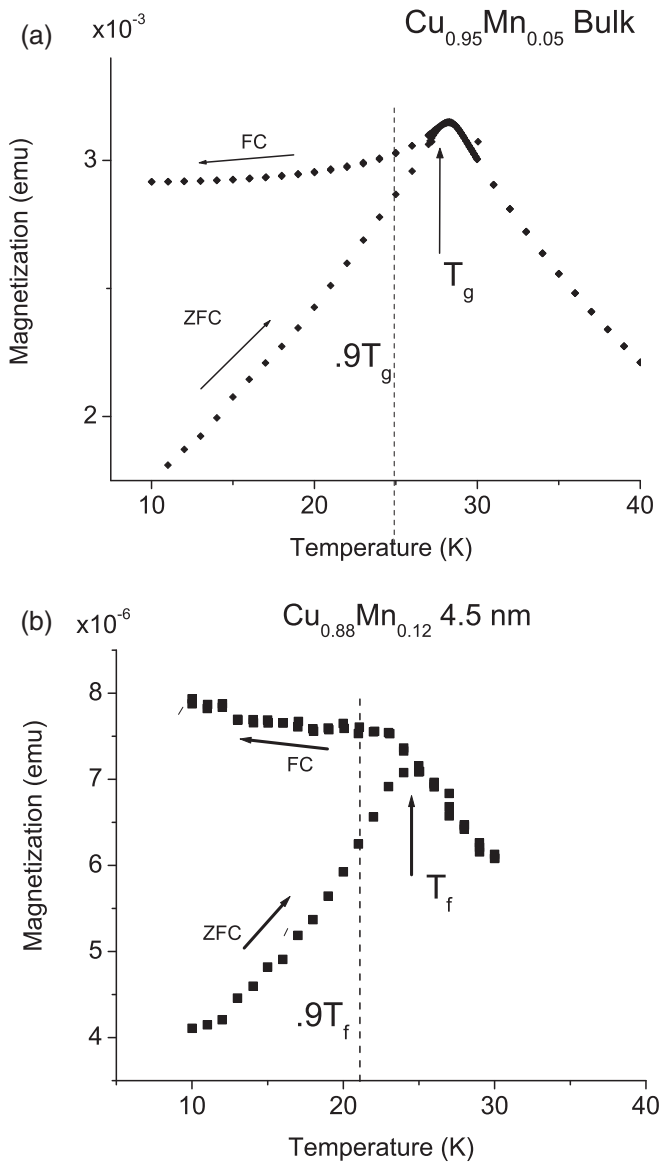


FIG. 1. (a) ZFC and FC magnetization curves in a 20 G magnetic field for bulk  $\text{Cu}_{0.95}\text{Mn}_{0.05}$ .  $T_g$  for the sample used in this study was determined to be 27.5 K. (b) ZFC and FC magnetization curves in 40 G for the multilayer  $\text{Cu}_{0.88}\text{Mn}_{0.12}$  (4.5 nm)/Cu (60nm). The bulk  $T_g$  for  $\text{Cu}_{0.88}\text{Mn}_{0.12}$  is 53 K, while  $T_f$  appears at 24.5 K.

for bulk samples, and  $T_f$  for thin films. Upon inspection of Fig. 1, the measurements of the FC-ZFC magnetizations versus temperature for both bulk and thin films look similar [4], but with important differences in the time dynamics. Sandlund *et al.* [9] measured the time dependent shift in the cusp of the magnetic susceptibility for both a bulk CuMn sample and a 3-nm CuMn thin film. They found that the bulk sample can be fitted with conventional critical dynamic scaling, and obtain a critical temperature within 1% of the measured FC susceptibility peak. This is in contrast with their thin film measurements. They found that a 3-nm film displayed more rapid dynamics that were inconsistent with critical dynamic scaling. Their data could be fitted, however, with a generalized Arrhenius law with a zero-temperature critical point.

Thermoremanent magnetization (TRM) experiments explore the decay of the irreversible component of the magnetization (i.e., the difference between the FC and ZFC magnetizations) as a function of temperature and waiting time. The conventional TRM experimental protocol is to apply a magnetic field at a temperature well above that for the onset of irreversibility, cool the sample through the transition temperature to the measurement temperature,  $T_m$ , wait (age) at  $T_m$  for a waiting time,  $t_w$ , then rapidly reduce the magnetic field to zero, and measure the time decay of the sample's magnetization. In general, the longer  $t_w$  is, the slower the decay of the TRM. In this sense, the effect of the waiting time is imprinted on the spin glass state, and directly observed through the TRM decay.

A straightforward method of observing the waiting time effect involves taking the logarithmic derivative of the magnetization decay  $S(t) = -dM(t)/d\ln t$ . In the temperature range  $0.4-0.9T_g$ , the  $S(t)$  function displays a peak at a time equal to the time where an inflection point in the decay is observed, which also happens to occur at a time approximately equal to the input waiting time.

For thin films, where the length scale is set by the film thickness  $\mathcal{L}$ , or bulk samples, where the length scale is set by the crystallite size, the cessation of aging, as extracted from the waiting time effect, provides direct evidence for domain growth in the spin glass phase. This explicitly ties aging in the spin glass state to an associated growth of the length scale for correlated spins. Previous studies have relied on the measurement of the maximum barrier height  $\Delta_{\max}(t_{\text{co}}, T)$  associated with the observed spin glass dynamics [14]. They were able to determine that  $\Delta_{\max}(t_{\text{co}}, T)$  was independent of temperature  $T$ . The connection to the saturation of the correlation length at  $\mathcal{L}$  for  $t > t_{\text{co}}$  was made only through the relationship connecting  $\Delta_{\max}(t, T)$  and  $\xi(t, T)$  established by Joh *et al.* using a hierarchical model [15]. Our approach relies only on the vanishing of the waiting time effect for TRM decay, and is therefore independent of a model-dependent analysis.

## II. EXPERIMENTAL TECHNIQUES

The bulk CuMn sample was made by ACI Alloys Inc. using 99.995% Cu and 99.95% Mn. At IUP, the sample was annealed at (900 °C) for 24 hours to randomize the Mn within the sample, followed by a rapid thermal quench to 77 K, to lock in the disorder. This standard procedure for producing highly disordered metallic spin glasses, however, has the effect of producing samples with small crystallites. Debye-Scherrer analysis of x-ray diffraction measurements (Fig. 2) of the bulk sample find a mean crystallite size of 80 nm. The measured transition temperature of 27.5 K implies a final bulk Mn concentration of approximately 5%. The  $\text{Cu}_{0.88}\text{Mn}_{0.12}/\text{Cu}$  multilayer sample consists of 40 bilayers of 4.5 nm of 99.9%  $\text{Cu}_{0.88}\text{Mn}_{0.12}$  separated by 60 nm of 99.999% Cu grown on a 2.54 cm  $\times$  5.08 cm Cu Foil. The sample was grown at the University of Minnesota and has been used in a multifaceted study of the mesoscopic spin glass phase. The multilayer film was dc sputtered at 2.0-mTorr Ar pressure, with a deposition rate of approximately 0.1 nm/s. A similarly prepared 1  $\mu\text{m}$  thick film was produced by sputtering onto a glass slide coated in photoresist. After sputtering, the photoresist was dissolved, and the resultant metal flakes were used

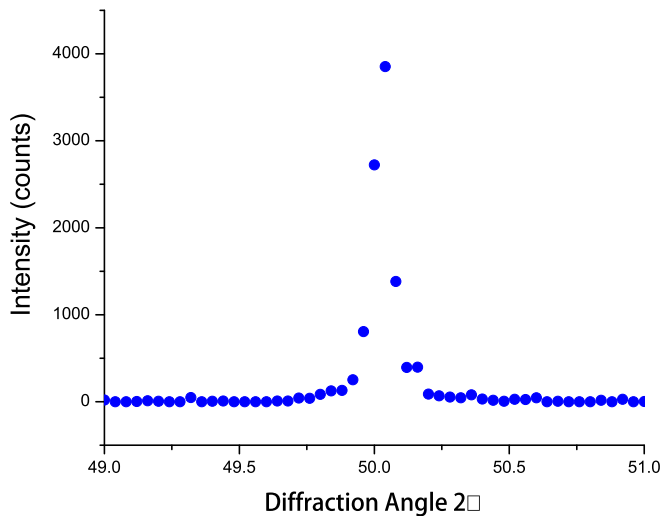


FIG. 2. The [200] peak of the x-ray diffraction pattern of the bulk  $\text{Cu}_{0.95}\text{Mn}_{0.05}$  sample.

to determine the bulk spin glass temperature,  $T_g = 53 \pm 1$  K. Scaling with respect to  $T_g$  indicates that the Mn concentration of our films is approximately 11.7 at.%.

The FC-ZFC data [Fig. 1(a)] were taken on the Quantum Design dc SQUID (QDDS) magnetometer at The University of Minnesota. The FC-ZFC data [Fig. 1(b)] were taken on the QDDS magnetometer at The University of Texas. It is well-known that the measurement of the spin glass transition temperature  $T_g$  is time dependent, shifting to lower temperatures for slower measurement techniques [9]. On these commercial magnetometers the FC-ZFC measurements take between 100–200 s per temperature point (corresponding to the time it takes for isothermal stabilization).

The Indiana University of Pennsylvania (IUP) ultrahigh sensitivity dual dc SQUID magnetometer was designed and built specifically to observe the time dependence of very small remnant magnetization, TRM, signals. Thin films spin glass samples have small signals because of sample size. Approaching the transition temperature both bulk spin glass samples and thin film samples have vanishingly small TRM signals as a consequence of the nature of the spin glass state.

The IUP magnetometer utilizes a dual dc SQUID configuration where one set of pickup coils houses the magnetic sample, while the other SQUID records environmental fluctuations. The sample sits in one of the two second order gradiometer pickup coils and is stationary for the entire measurement of the decay. Each pickup coil is inductively coupled to an independent SQUID amplifier. The sample is attached to the bottom of a 36-cm sapphire rod. The sample heater is located near the top of the sapphire rod. For the thin film and bulk data  $\leq 24$  K, the measurement thermometer (user calibrated Lakeshore Cryogenics Cernox temperature sensor), was located on the sapphire rod 10 cm above the sample. For bulk data,  $> 24$  K, a Lakeshore calibrated Cernox temperature sensor was placed on the sapphire rod approximately 2 mm above the sample. All temperature data presented were calibrated to the Lakeshore calibrated thermometer. The entire rod and sample are wrapped in teflon tape with the exception of an approximately 10 cm region at the top of the sapphire

rod to improve heat exchange with the He bath through He exchange gas introduced into the doubled-walled vacuum jacket surrounding the sample probe. While this configuration is not the most efficient for helium consumption, it is thermally very stable and allows rapid (within a few tens of seconds) change and stabilization of the temperature. Fast Cooling protocols [12] were employed for the TRM measurements, reaching a stable measurement temperature  $T_m$  within 30–50 s of the temperature quench. The temperature at  $T_m$  was monitored continuously and found to be stable to a standard deviation of  $\pm 0.6$  mK over the entire duration of the measurement, 40 000 s. TRM measurements were performed using a magnetic field of 20 G, on both the bulk and multilayer samples over a wide range of temperatures and waiting times.

Commercial magnetometers physically move the sample through the pickup coils for every measurement integrating the entire sample signal and therefore each point is measured as an absolute measurement of the sample magnetization. In the IUP magnetometer, an absolute magnetization point is taken only once at the end of the decay. Immediately following the TRM measurement, the temperature is raised above  $T_g$  and then re-cooled to  $T_m$ , all in the absence of the magnetic field, at which point a baseline magnetization is measured. The difference between all of the points of the remanent decay (40 000 s) and the baseline provides an absolute value determination for the remanent magnetization decay at that time. As an absolute magnetization measurement, the last point is the most accurate experimental point as other points along the decay are further separated in time from the baseline point and hence are more affected by long time noise and drifts. We therefore have standardized our total measurement time to 40 000 s for all samples and temperatures. This allows for the comparison of the most accurate remanence measurements between different waiting times, temperature runs, and different samples. While 40 000 s may seem arbitrary we chose this timescale for several reasons. First, it is significantly larger than any of the waiting times used and therefore not obviously in the region of the standard waiting time effect. Second, this timescale is in the region where we have previously observed end of aging effects. Finally, it is convenient, taking approximately 12 hour per run and allowing for the fully automated acquisition of 4–5 full measurements between He fills.

A disadvantage of using a single SQUID in a stationary sample measurement protocol is the presence of low frequency environmental noise [9,16]. In particular, once we were able to resolve signals in the thin film sample down to the  $1 \times 10^{-8}$  emu level, we found a direct coupling between the atmospheric pressure and the SQUID signal. During these measurements, the helium liquid was directly vented through a long thin tube to atmospheric pressure. Long time drifts (hours to days) of the atmospheric pressure produced drifts as large as  $1 \times 10^{-7}$  emu over measurement times as long as 40 000 s. In the thin-film data, we were able to unambiguously remove these drifts by subtraction of the environmental fluctuation SQUID signal, from the magnetic sample SQUID signal. This, coupled with the smaller pickup coil diameter (1.1 cm) (approximately 1/2 the QDDS) resulted in a significant enhancement of the signal to noise ratio as compared to commercial SQUIDs. We have since decreased this extraneous

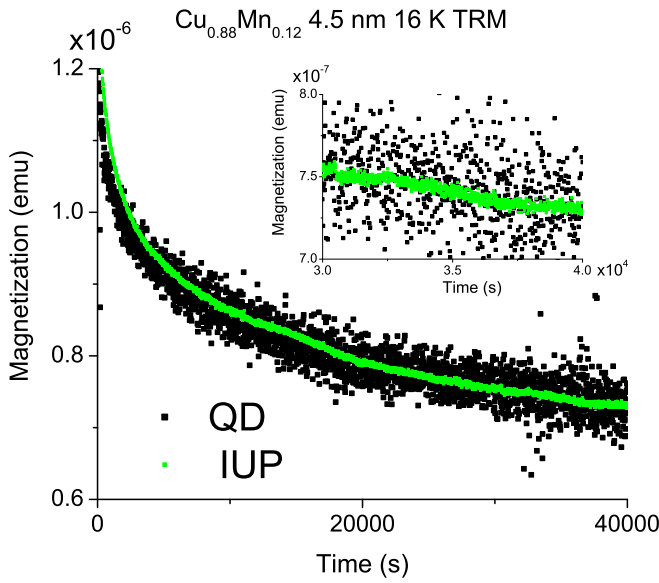


FIG. 3. Calibration and comparison runs for UT Quantum Design dc SQUID magnetometer and IUP ultrahigh sensitivity dc SQUID magnetometer. Signal comparison was made at 16 K on the same  $\text{Cu}_{0.88}\text{Mn}_{0.12}$  (4.5 nm)/Cu (60 nm) multilayer sample.

signal, by approximately an order of magnitude, by isolating the helium bath from the atmosphere and rigidly controlling gas flow pressure from the dewar to the atmosphere. This reduced noise technique was also applied to the bulk sample decay data presented here. For a more complete description of the IUP magnetometer, see Ref. [17].

Figure 3 displays the calibration run between the IUP device and the QDDS magnetometer at the University of Texas at Austin. The calibration runs were made on the same

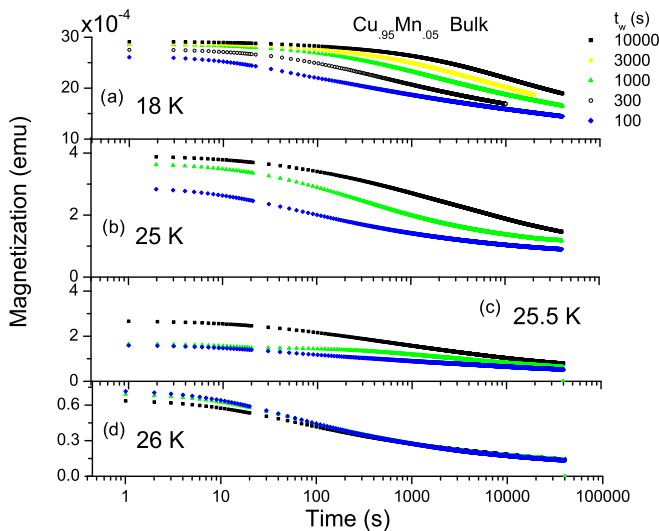


FIG. 4. Waiting times range from 100 to 10 000 s for all temperatures. (a) Thermoremanent magnetization (TRM) decays of the bulk  $\text{Cu}_{0.95}\text{Mn}_{0.05}$  sample at 18 K ( $0.65T_g$ ). (b) TRM decays of the bulk  $\text{Cu}_{0.95}\text{Mn}_{0.05}$  sample at 25 K ( $0.91T_g$ ). (c) TRM decays of the bulk  $\text{Cu}_{0.95}\text{Mn}_{0.05}$  sample at 25.5 K ( $0.93T_g$ ). (d) TRM decays of the bulk  $\text{Cu}_{0.95}\text{Mn}_{0.05}$  sample at 26 K ( $0.95T_g$ ).

sample. In general, during the measurement of the magnetization decay data, the IUP magnetometer samples an analog signal once every second. The QD system samples an absolute value of the magnetization by moving the sample up and down through the pickup coils. This measurement takes approximately 10 s. For a more direct comparison, we therefore compare by averaging our data over 10 s intervals. The data is calibrated by comparing the average of the last 1000 s of the 40 000 s decays (Fig. 3), and determining a multiplication factor. This multiplication factor is used for all of the data presented. We find that the IUP magnetometer exhibits a point to point resolution more than an order of magnitude better than the commercial DC SQUID magnetometer. While this calibration factor worked well for the thin film, we find in the bulk sample that it produces remanences that are smaller in the IUP magnetometer than what is expected from the FC/ZFC curves. We believe that in the stationary measurement protocol only a small portion of the 1-cm-long sample actually sits in top coil of the pickup coils and therefore a smaller portion of the sample is actually measured.

### III. EXPERIMENTAL RESULTS

#### A. Bulk CuMn

Figure 4 displays bulk sample TRM decays for waiting times ranging from 100 to 10 000 s and for temperatures of 18 K ( $0.65T_g$ ), 25 K ( $0.91T_g$ ), 25.5 K ( $0.93T_g$ ), and 26 K ( $0.95T_g$ ). The 18-K data display standard decays and waiting time effects that have been extensively investigated [9, 18–20]. The data for temperatures higher than  $0.9T_g$  display deviations from the lower temperature decays with the differences increasing as the transition temperature is approached. While the size of the remnant decay decreases with increasing temperature, the baseline point (the last point taken at 40 000 s) approaches zero as expected from the FC/ZFC curve in Fig. 1.

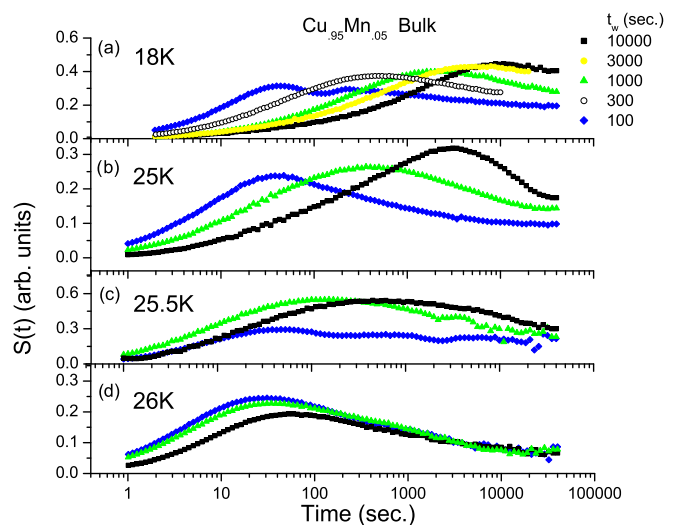


FIG. 5. Waiting times range from 100 s to 10 000 s for all temperatures. (a)  $S(t)$  of the bulk  $\text{Cu}_{0.95}\text{Mn}_{0.05}$  sample at 18 K. (b)  $S(t)$  of the bulk  $\text{Cu}_{0.95}\text{Mn}_{0.05}$  sample at 25 K. (c)  $S(t)$  of the bulk  $\text{Cu}_{0.95}\text{Mn}_{0.05}$  sample at 25.5 K. (d)  $S(t)$  of the bulk  $\text{Cu}_{0.95}\text{Mn}_{0.05}$  sample at 26 K.



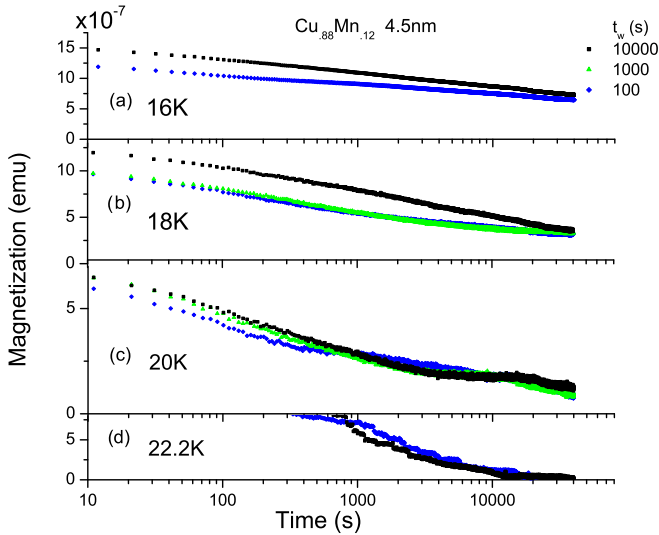


FIG. 6. Waiting times range from 100 to 10 000 s for all temperatures. (a) Thermoremanent magnetization decays (TRM) decays of the multilayer  $\text{Cu}_{0.88}\text{Mn}_{0.12}$  (4.5 nm)/ Cu (60 nm) sample at 16 K. (b) TRM decays of the  $\text{Cu}_{0.88}\text{Mn}_{0.12}$  (4.5 nm)/ Cu (60 nm) sample at 18 K. (c) TRM decays of the  $\text{Cu}_{0.88}\text{Mn}_{0.12}$  (4.5 nm)/ Cu (60 nm) sample at 20 K. (d) TRM decays of the  $\text{Cu}_{0.88}\text{Mn}_{0.12}$  (4.5 nm)/ Cu (60 nm) sample at 22.2 K.

The inflection points appear to shift down in time as the temperature increases. At  $0.95T_g$ , at long times, the curves collapse on each other and we are not able to discern a waiting time effect. This is very similar to the end of aging effect observed at  $0.83T_g$  [21], where the effect of the time, the sample ages at the waiting time, is no longer evident in the long-time region of the decay and all remnant decay occurs along a single curve. The main difference is that, in the previous study, end of aging was observed only for very short waiting times. In this study, as the transition temperature is approached, end of aging is observed for waiting times as long as 10 000 s.

Figure 5 displays the  $S(t) = -dM(t)/d\ln t$  functions for the TRM decays of Fig. 4. Below approximately  $0.9 T_g$  the peaks in the  $S(t)$  functions display a peaks at a temperature approximately equal to the waiting time. We find that as the temperature increases above  $0.9 T_g$ , the peaks systematically shift to shorter timescales. For example, in Fig. 5(c) at 25.5 K ( $0.93T_g$ ), the peak in the 10 000 s and the 1000 s curves has shifted down in time by an order of magnitude. At 26 K ( $0.95T_g$ ), the peaks in the 10 000 s and the 1000 s curves have shifted down to less than 100 s. A full discussion and analysis of the  $S(t)$  function over the entire temperature range will be presented in a separate follow up report.

### B. CuMn 4.5-nm thin films

Figure 6 displays the 4.5-nm-thin-film TRM decays for temperatures of 16 K ( $0.65T_f$ ), 18 K ( $0.73T_f$ ), 20 K ( $0.81T_f$ ), and 22.2 K ( $0.91T_f$ ) and waiting times ranging from 100 to 10 000 s. In agreement with previous measurements, the TRM in the thin films does not show the obvious waiting time structure of the bulk samples (i.e., an inflection point) well into the spin glass phase [Fig. 6(a)] [9]. We do, however,

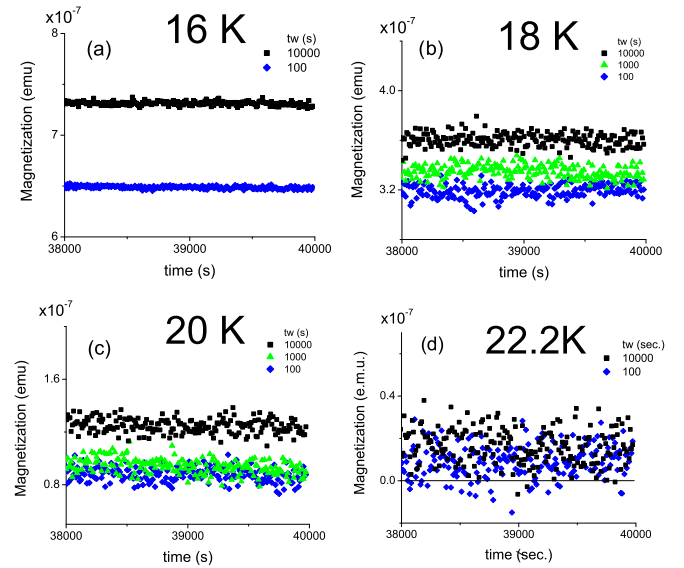


FIG. 7. The last 2000 s of the remanent decay taken (a) 16, (b) 18, (c) 20, and (d) 22.2 K.

observe a waiting time effect in the shift of the decays in the 16- and 18-K measurements. We also observed that at 40 000 s. There is still a significant remnant moment that also displays a waiting time dependent shift. At 20 K, we are not able to discern differences between the long time decays, likely because of the previously mentioned drifts. We do, however, still see a waiting time effect at 20 K, in the remanence at 40 000 s [Fig. 7(c)]. While the 22-K data have a large drift at short times, the last 25 000 s are stable and we could still measure an accurate baseline.

In Fig. 7, we expand the last 2000 s of the thin film TRM decays for temperatures of 16, 18, 20, and 22.2 K. The waiting time effect is apparent from a waiting time dependent shift in these curves. Figure 7 suggests a method for comparing the waiting time effect in samples that do not display obvious bulk waiting time structure.

## IV. DISCUSSION

The question arises as to how we compare the decays observed in the bulk data with the decays observed in the thin films. The bulk data have a definitive structure that reflects the waiting time, and can readily be observed in the peak in the  $S(t)$  function. At high temperatures, this structure disappears and all of the discernible waiting time effects also disappear. However, there is still a TRM decay, and an apparent waiting time independent (at least below our ability to resolve) remanent behavior. The thin-film data show no such structure. The thin-film data, however, do show a waiting time effect in the separation of the curves and final remanence at 40 000 s. These differences notwithstanding, we can compare waiting time effects in the bulk sample at different temperatures and in different types of samples by comparing the final remanence.

In Fig. 8(a), we plot the final point for each of the bulk sample TRM decay curves at 40 000 s at a variety of different measuring temperatures. In Fig. 8(b), we plot the final point for each of the thin film sample TRM decay curves at 40 000 s

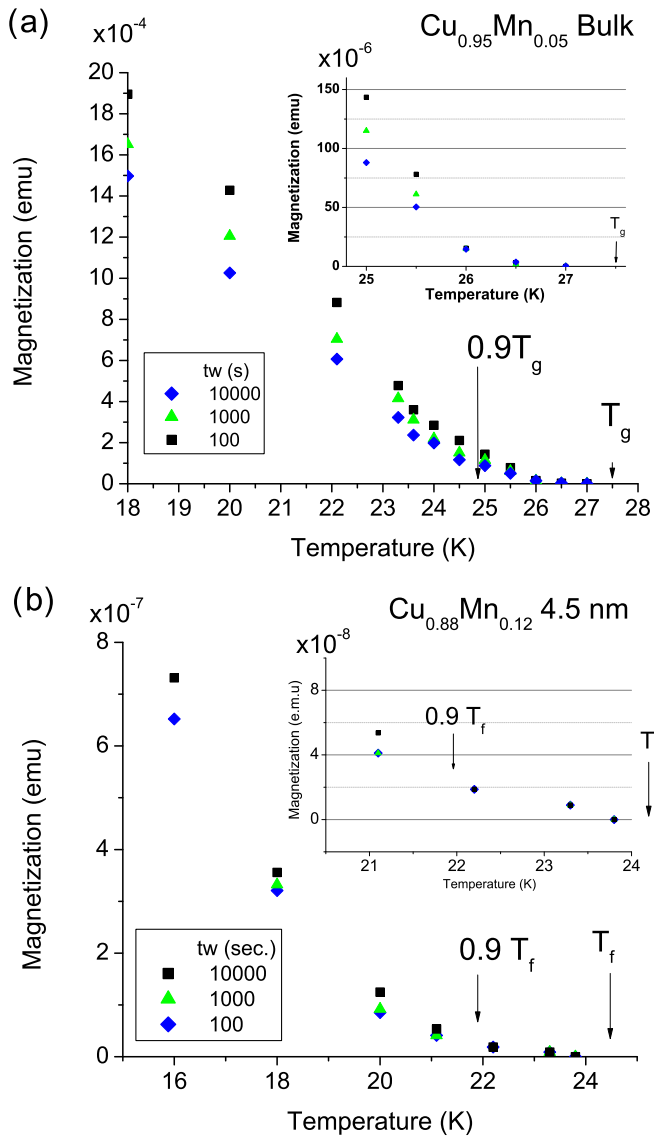


FIG. 8. (a) Remanence taken at 40 000 s for bulk  $\text{Cu}_{0.95}\text{Mn}_{0.05}$ .  $T_g$  for  $\text{Cu}_{0.95}\text{Mn}_{0.05}$  is 27.5 K. (b) Remanence taken at 40 000 s for a multilayer  $\text{Cu}_{0.88}\text{Mn}_{0.12}$  (4.5 nm)/ Cu (60 nm). Bulk  $T_g$  for the  $\text{Cu}_{0.88}\text{Mn}_{0.12}$  is 53 K, while  $T_f$  appears at 24.5 K.

at a variety of different measuring temperatures. The waiting time effect is observed as a systematic waiting time dependent shift in the 40 000 s remanent behavior. In the bulk sample, we observe that the waiting time effect persists for temperatures up to  $0.96T_g$ . In the thin film sample, at approximately  $0.9T_f$ , the waiting time effect disappears. We do not observe a difference either in the decay curves or in the final remanent point. There is, however, still a waiting time independent remanence which decreases to zero when the temperature is increased. This remanence indicates that we are still in the spin glass phase but in a waiting time independent region (end of aging) [21].

These results are evidence that the correlation length,  $\xi(t, T)$ , grows with time until  $\xi_{\perp}(t, T)$  has reached the film thickness for the thin film [5], or the crystallite size for the bulk sample [12]. Once this limit is reached, the growth ends

and a quasiequilibrium state is maintained with  $\xi_{\perp}(t_{\text{co}}, T) = \mathcal{L}$ . Aging ceases, and the TRM decays independent of waiting times longer than  $t_{\text{co}}$ .

Although our results are not model dependent, we can compare our results with a model to demonstrate consistency. Previously [12], we utilized a model based on numerical simulations [5] using a four-spin correlation length to explain spin glass dynamics data. This model includes a correlation length within the spin glass state,  $\xi(t, T)$ , that grows with time. Four important externally controlled parameters define spin glass experiments: temperature, magnetic field, time, and length scale. Extensive waiting time and temperature cycling measurements have linked the first three of these in the bulk [15], leading to the development of a model of the spin glass state that relies on the growth of a four-spin correlation length [15]. The model has successfully linked the above four parameters [5,12] using a correlation length whose growth with time was extracted from numerical simulation studies [22]:

$$\xi(t, T) = c_1 a_0 \left( \frac{t}{\tau_0} \right)^{c_2 (T/T_g)}, \quad (1)$$

where  $a_0$  is an average distance between magnetic ions,  $T_g$  is the bulk transition temperature,  $\tau_0$  is the microscopic exchange time, and  $c_1$  and  $c_2$  are material-dependent constants.

One can determine a value for  $t_{\text{co}}$  from Fig. 8 by identifying the temperature at which the magnetization data collapse for different waiting times, and setting the shortest waiting time at that temperature as  $t_{\text{co}}$ . By using the two different thicknesses, 80 nm for the bulk, and 4.5 nm for the thin film, in Eq. (1), and the relevant  $t_{\text{co}}$  from Fig. 8, we can solve for  $c_1$  and  $c_2$ . For the bulk, we take the collapse to occur at  $T = 26.25$  K,  $t_{\text{co}} = 100$  s, and  $\mathcal{L} = 80$  nm. For the thin film, we take the collapse to occur at  $T = 22.2$  K,  $t_{\text{co}} = 100$  s, and  $\mathcal{L} = 4.5$  nm. The microscopic exchange rate for the thin film is  $1/\tau_0 = 6.9 \times 10^{12} \text{ s}^{-1}$  corresponding to an average separation between Mn atoms of  $a_0 = 0.523$  nm for a Mn concentration of 12 at.%. The bulk sample used in this paper has a Mn concentration of 5 at.%, so scaling by concentration results in  $1/\tau_0 = 3.6 \times 10^{12} \text{ s}^{-1}$  and  $a_0 = 0.691$  nm. Equation (1) then results in  $c_1 = 1.070$  and  $c_2 = 0.147$ . These values are close to previous ones [5], and to those found from simulations [22].

In summary, for two different spin glass samples, one bulk and one thin film with different concentrations, we have demonstrated that aging is representative of domain growth without resort to a specific model for the dynamics. We also have shown that our results are consistent with an algebraic growth model, establishing values for the coefficients that predict the timescales for the growth of spin glass correlations. We believe these results establish the existence of the spin glass correlation length, and its dependence on time and temperature.

## ACKNOWLEDGMENTS

This work was supported by the US Department of Energy, Office of Science, Basic Energy Sciences, under Award DE-SC0013599. The IUP dual dc SQUID magnetometer was built under an NSF MRI, Award No. 0852643.

- [1] V. Cannella and J. A. Mydosh, *Phys. Rev. B* **6**, 4220 (1972).
- [2] S. F. Edwards and P. W. Anderson, *J. Phys. F* **5**, 965 (1975).
- [3] S. A. Werner, *Solid State Commun.* **56**, 457 (1985).
- [4] G. G. Kenning, J. M. Slaughter, and J. A. Cowen, *Phys. Rev. Lett.* **59**, 2596 (1987); G. G. Kenning, J. Bass, W. P. Pratt, Jr., D. Leslie-Pelecky, L. Hoines, W. Leach, M. L. Wilson, R. Stubi, and J. A. Cowen, *Phys. Rev. B* **42**, 2393 (1990).
- [5] Q. Zhai, D. C. Harrison, D. Tennant, E. D. Dalhberg, G. G. Kenning, and R. L. Orbach, *Phys. Rev. B* **95**, 054304 (2017).
- [6] L. Hoines, J. A. Cowen, and J. Bass, *J. Appl. Phys.* **79**, 6151 (1996); *Physica B* **194**, 309 (1994); R. Stubi, J. A. Cowen, D. Leslie-Pelecky, and J. Bass, *Phys. Rev. B* **44**, 5073 (1991).
- [7] M. Sawicki, T. Dietl, T. Skoskiewicz, G. Karczewski, T. Wojtowicz, and J. Kossut, *Acta Phys. Pol. A* **88**, 1038 (1995).
- [8] C. Dekker, A. F. M. Arts, H. W. de Wijn, A. J. van Duyneveldt, and J. A. Mydosh, *Phys. Rev. Lett.* **61**, 1780 (1988).
- [9] L. Sandlund, P. Granberg, L. Lundgren, P. Nordblad, P. Svedlindh, J. A. Cowen, and G. G. Kenning, *Phys. Rev. B* **40**, 869 (1989).
- [10] S. Franz, G. Parisi, and M. A. Virasoro, *J. Phys. I (France)* **4**, 1657 (1994).
- [11] I. Morgenstern and K. Binder, *Phys. Rev. Lett.* **43**, 1615 (1979).
- [12] S. Guchhait, G. G. Kenning, R. L. Orbach, and G. F. Rodriguez, *Phys. Rev. B* **91**, 014434 (2015).
- [13] Q. Zhai, D. C. Harrison, and R. L. Orbach, *Phys. Rev. B* **96**, 054408 (2017).
- [14] S. Guchhait and R. Orbach, *Phys. Rev. Lett.* **112**, 126401 (2014).
- [15] Y. G. Joh, R. Orbach, G. G. Wood, J. Hammann, and E. Vincent, *Phys. Rev. Lett.* **82**, 438 (1999).
- [16] J. Clarke and A. I. Braginski, *The SQUID Handbook* (Wiley, Weinheim, 2004), Sec. 5.6.
- [17] Daniel Tennant, Ph.D. Thesis, University of Texas Austin, 2017.
- [18] M. Alba, J. Hammann, M. Ocio, and Ph. Refregier, H. Bouchiat, *J. Appl. Phys.* **61**, 3683 (1987).
- [19] G. G. Kenning, J. Bowen, P. Sibani, and G. F. Rodriguez, *Phys. Rev. B* **81**, 014424 (2010).
- [20] G. F. Rodriguez, G. G. Kenning, and R. Orbach, *Phys. Rev. B* **88**, 054302 (2013).
- [21] G. G. Kenning, G. F. Rodriguez, and R. Orbach, *Phys. Rev. Lett.* **97**, 057201 (2006).
- [22] H. Rieger, *J. Phys. A: Math. Gen.* **26**, L615 (1993); H. Rieger, B. Steckemetz, and M. Schreckenberg, *Europhys. Lett.* **27**, 485 (1994).

*Correction:* The surname of the eighth author contained a typographical error and has been fixed.